Preliminary Evaluation of 15-[^{18}F]Fluoro-3-oxa-pentadecanoate as a PET Tracer of Hepatic Fatty Acid Oxidation

Timothy R. DeGrado, Shuyan Wang, and Donald C. Rockey

Departments of Radiology and Medicine, Duke University Medical Center, Durham, North Carolina

The liver is an important site of fat oxidation. Abnormalities of hepatic mitochondrial fatty acid oxidation (HMFAO) are associated with obesity, type II diabetes, alcoholic hepatitis, and nonalcoholic steatohepatitis. Noninvasive assessment of HMFAO by PET has been impeded by the lack of a specific radiotracer. **Methods:** No-carrier-added 15-[^{18}F]fluoro-3-oxa-pentadecanoate (FOP) was synthesized and evaluated in living rats and isolated rat livers. **Results:** FOP showed high uptake and slow clearance of radioactivity from livers in living rats. Inhibition of HMFAO by pretreatment of fasting rats with the carnitine palmitoyltransferase-I (CPT-I) inhibitor reduced the liver-to-blood ratio by 64%. In isolated rat livers, perfused in normoxic (95% O_2) and hypoxic (15% O_2) conditions with glucose (5 mmol/L) and palmitate (0.15 mmol/L), the externally measured kinetics of FOP showed reversible binding in tissue. The kinetics were adequately fit by a catenary 2-compartment model for estimation of tracer distribution volumes (DVs). The DVs of both compartments were found to correlate with fractional palmitate oxidation rate (FPOR) in experiments in normoxic and hypoxic conditions. The correlation was particularly strong for the slower second compartment (DV_2 [mL/g dry weight] = 34.1 FPOR [mL/min/g dry weight] − 0.7, r = 0.89). Relatively small levels of diffusible metabolites of FOP were formed in vivo and in isolated rat liver. **Conclusion:** The selective uptake of FOP by liver and the high sensitivity of hepatic FOP DV to changes of HMFAO with CPT-I inhibition and hypoxia suggests potential usefulness for the 3-oxa fatty acid analog in assessments of hepatic mitochondrial oxidation of exogenous fatty acids with PET. These data emphasize that further studies are required to clarify the intracellular disposition of FOP in the liver and test its validity as a tracer of HMFAO over a broad range of conditions.

Key Words: liver; fatty acids; β-oxidation; PET

J Nucl Med 2000; 41:1727–1736

The liver is an important site of fat oxidation. Although disturbance of hepatocyte fatty acid metabolism with an abnormally high accumulation of triglycerides is a common feature of both alcoholic hepatitis and nonalcoholic steatohepatitis (NASH), the biochemical pathogenesis of these fatty liver diseases is poorly understood. Animal models of alcoholic steatosis are of limited value (*1*), and an animal model of NASH does not exist. Inhibition of mitochondrial β-oxidation is thought to contribute to triglyceride accumulation in alcoholic fatty liver (*1*) and NASH (*2*). Disorders of hepatic mitochondrial fatty acid oxidation (HMFAO) are also associated with obesity (*3*,*4*) and type II diabetes (*5*,*6*). However, noninvasive evaluation of regional HMFAO in liver by an imaging technique has proven problematic.

The availability of both anabolic and catabolic metabolic pathways for fatty acids in liver complicates the design and implementation of a tracer technique to measure oxidative metabolic flux. The use of [1-^{11}C]octanoate (OA) for assessing mitochondrial β-oxidation in liver using PET has been proposed on the basis of hepatic clearance rates of ^{11}C-radioactivity presumably reflecting oxidation of the tracer and clearance of $^{11}CO_2$ (*7*). However, β-oxidation of OA presumably gives rise to [1-^{11}C]acetyl coenzyme A (CoA), which has both anabolic and catabolic metabolic fates in liver. Retention of anabolic metabolites of [1-^{11}C]acetyl-CoA would cause an underestimation of β-oxidation activity by clearance rates of radioactivity from liver. Modified fatty acid analogs that are retained specifically as β-oxidation metabolites would have more potential to serve as radiolabeled probes of fatty acid oxidation. Toward this end, β-methyl- and acetylene-substituted analogs of OA have been synthesized and show prolonged retention in liver (*8*). However, the specificity of these analogs for indication of β-oxidation activity has not been clarified.

We are investigating sulfur and oxygen heteroatom substituted fatty acid analogs as metabolically retained probes of HMFAO in liver. We have recently developed the 4-thia palmitate analog, 16-[^{18}F]fluoro-4-thia-hexadecanoic acid ([FTP] Fig. 1), as a metabolically trapped tracer of mitochondrial fatty acid oxidation in the heart used in conjunction with PET (*9*,*10*). However, preliminary work in isolated rat liver showed that β-oxidation–independent metabolic trapping of FTP in liver limits the usefulness of FTP as a probe of HMFAO (*11*).

Skorve et al. (*12*) have shown that feeding a 3-oxa long-chain fatty acid to rats leads to a greater than 97% inhibition of palmitoyl-L-carnitine oxidation in liver mito-

Received Aug. 19, 1999; revision accepted Mar. 2, 2000.

For correspondence or reprints contact: Timothy R. DeGrado, PhD, Duke University Medical Center, Department of Radiology, Box 3949, Durham, NC 27710.

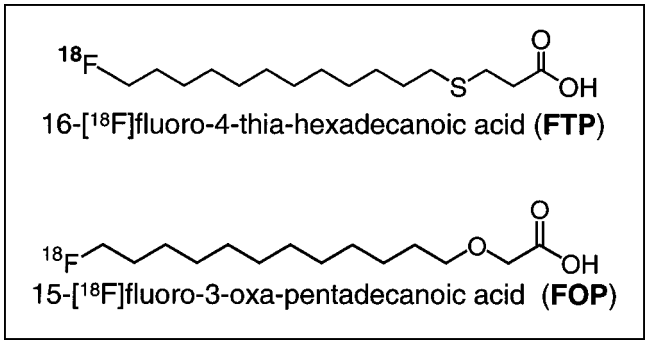

FIGURE 1. Chemical structures of ^{18}F-labeled fatty acids.

chondria. The mechanism of inhibition of β-oxidation by 3-oxa fatty acids has not been clarified, but a reasonable possibility is an accumulation of a metabolite, such as the corresponding acyl-CoA or acylcarnitine, that inhibits 1 or more enzymes of HMFAO. For this reason, we postulated that a radiolabeled 3-oxa fatty acid would likely be retained in liver mitochondria (i.e., in relationship with acyl intermediates of the HMFAO pathway). This study evaluated the potential usefulness of an ^{18}F-labeled 3-oxa fatty acid, 15-[^{18}F]fluoro-3-oxa-pentadecanoate (FOP; Fig. 1), as a probe of mitochondrial β-oxidation in liver.

MATERIALS AND METHODS

Synthesis of Radiotracers

Chemicals were of analytic grade. Dry acetonitrile was obtained commercially (Pierce, Rockford, IL). ^{1}H-nuclear magnetic resonance (NMR) spectra were recorded with a 500-MHz Unity spectrometer (Varian, Inc., Palo Alto, CA) using $CDCl_3$ as the solvent (Me_4Si, 0.00 ppm). R_f values refer to thin-layer chromatography (TLC) performed on silica gel with the solvent system noted. Routine column chromatography was performed under normal pressure with silica gel (100–200 mesh) and the solvent system noted.

Methyl 15-Hydroxy-3-oxa-pentadecanoate

12-Tetrahydropyranyloxy-1-dodecanol was synthesized from 1,12-dodecanediol as previously described (*13*). This alcohol (5 mmol) was caused to react with *t*-butyl bromoacetate (20 mmol) and tetrabutylammonium hydrogen sulfate (5 mmol) in 20 mL 50% NaOH and 15 mL CH_2Cl_2 at room temperature for 4 h according to a previously described procedure (*14*). The solution was extracted twice with ether, and the organic phase was dried ($MgSO_4$) and evaporated under reduced pressure. The product of this reaction, *t*-butyl 15-tetrahydropyranyloxy-3-oxa-pentadecanoate, was isolated by liquid chromatography (hexane:ethyl acetate, 3:1; R_f = 0.7). This product was directly caused to react in methanol with a catalytic amount of p-toluenesulfonic acid for 6 h at reflux. After neutralization of the solution with sodium bicarbonate, the solvent was evaporated. Ether (20 mL) and brine (20 mL) were added, and the organic layer was dried ($MgSO_4$) and evaporated under reduced pressure. The product, methyl 15-hydroxy-3-oxa-pentadecanoate (2.3 mmol, 46%), was isolated as a colorless oil by liquid chromatography (hexane:ethyl acetate, 7:3; R_f = 0.3). ^{1}H-NMR 1.2–1.65 (m, 20H, CH_2), 3.52 (t, 2H, C(4)H_2), 3.64 (t, 2H, C(15)H_2), 3.76 (s, 3H, -$COOCH_3$), 4.08 (s, 3H, C(2)H_2).

Methyl 15-Iodo-3-oxa-pentadecanoate

To 2.1 mmol methyl 15-hydroxy-3-oxa-pentadecanoate in *N,N*-dimethylformamide (5 mL) was added 2.5 mmol triphenylphosphine, and the solution was stirred at room temperature for 5 min. To this solution was added iodine crystals until a reddish color persisted, indicating completeness of reaction. Ether (20 mL) and water (20 mL) were added, and the organic layer was washed successively with water and brine, dried ($MgSO_4$), and evaporated under reduced pressure. The product, methyl 15-iodo-3-oxa-pentadecanoate, was isolated as an oil in 90% yield by column chromotography (hexane:ethyl acetate, 3:1). TLC (hexane:ethyl acetate, 3:1; R_f = 0.7) ^{1}H-NMR 1.2–1.65 (m, 20H, CH_2), 3.19 (t, 2H, C(15)H_2), 3.52 (t, 2H, C(4)H_2), 3.76 (s, 3H, -$COOCH_3$), 4.08 (s, 3H, C(2)H_2). The compound was stable when kept at 5°C.

[^{19}F]Fluoro-3-oxa-pentadecanoic Acid

To 5 mL of a 1 mol/L solution of tetrabutylammonium fluoride in tetrahydrofuran was added 1.15 mmol methyl 15-iodo-3-oxa-pentadecanoate. The solution was stirred at room temperature for 4 h. Ether (20 mL) and water (20 mL) were added, and the organic phase was dried ($MgSO_4$) and evaporated under reduced pressure. The resultant fluoroester was isolated by column chromatography (hexane:ethyl acetate, 3:1). TLC (hexane:ethyl acetate, 3:1) showed an R_f of 0.4. The fluoroester was directly hydrolyzed in 20 mL ethanol and 0.2-N KOH (1:1) at room temperature overnight. After evaporation of most of the ethanol, ether (30 mL) and dilute HCl were added. The organic layer was washed with brine, dried ($MgSO_4$), and evaporated under reduced pressure. The product, 15-[^{19}F]fluoro-3-oxa-pentadecanoic acid, was crystallized in 60% yield from hexane (melting point = 38°C). ^{1}H-NMR 1.2–1.65 (m, 20H, CH_2), 3.52 (t, 2H, C(4)H_2), 4.08 (s, 3H, C(2)H_2), 4.44 (dt, 2H, C(15)H_2, J_{HF} = 47.5 Hz, J_{HH} = 6.2 Hz).

^{18}F-Labeling Procedure

The radiofluorination procedure was that of DeGrado (*15*), as modified from that of Coenen et al. (*16*). The precursor for ^{18}F-labeled FOP was methyl 15-iodo-3-oxa-pentadecanoate. To a 2-mL glass vial was added Kryptofix 2.2.2 (10 mg; Aldrich, Milwaukee, WI), acetonitrile (0.5 mL), and a 9% K_2CO_3 solution in water (20 μL). [^{18}F]fluoride, produced through proton bombardment of $H_2{}^{18}O$ (>95 atom %), was then added; the vessel was placed in an aluminum heating block at 85°C; and the solvent was evaporated under a stream of helium or nitrogen. The residue was further dried by azeotropic distillation with acetonitrile (2 × 0.3 mL). A solution of methyl 15-iodo-3-oxa-pentadecanoate (1–2 mg) in acetonitrile (0.5 mL) was added, and the vial was sealed and returned to the heating block. Reaction time was 10 min. The vial was briefly cooled by placing it in ice water. The incorporation of [^{18}F]fluoride was monitored by radio-TLC (hexane:ethyl acetate, 3:1). R_f values were 0.0 and 0.6 for [^{18}F]fluoride and [^{18}F]fluoroester, respectively.

Subsequent hydrolysis of the resulting [^{18}F]fluoroester was performed in the same vessel by the addition of 0.15 mL 0.2-N KOH and continued heating at 90°C for 4 min. The mixture was cooled, acidified with concentrated acetic acid (25 μL), and applied to a semipreparative reverse-phase high-performance liquid chromatography (HPLC) column (Nuclosil C-18 [10 μ, 250 × 10 mm]; Alltech, Deerfield, IL) eluted with MeOH:H_2O:AcOH (85:14.5:0.5) at a flow rate of 4.3 mL/min. The HPLC capacity factors (k′) were 3.1 and 5.2 for FOP and the hydrolyzed precursor, 15-iodo-3-oxa-pentadecanoate, respectively. An in-line ultraviolet-detector (210 nm) was used to monitor the elution of unlabeled materials.

The [^{18}F]fluoro–fatty acid fraction was collected, evaporated to dryness, formulated in isotonic NaCl solution with 1%–2% albumin present, and filtered through a 0.22-μm filter (Millex-GS; Millipore, Bedford, MA).

Biodistribution Studies in Rats

Female Sprague-Dawley rats (body weight range, 180–225 g) fasted overnight. The rats were anesthetized with pentobarbital (75 mg/kg) before injection of the radiotracer and remained anesthetized throughout the study. The ^{18}F-labeled FOP (20–40 μCi) was injected into the femoral vein. A prescribed duration was allowed before procurement of tissues (heart, liver, lung, blood, kidney, bone [rib], brain [whole], skeletal muscle, and urinary bladder). The tissues were counted and weighed. Radioactivity data were corrected for decay. Radiotracer uptake was calculated as:

$$\text{Uptake (\% dose kg/g)} = \frac{(\%\ \text{injected dose})(\text{rat weight [kg]})}{\text{tissue mass (g)}}. \qquad \text{Eq. 1}$$

In one group of fasting rats, the carnitine palmitoyltransferase I (CPT-I) inhibitor, etomoxir (40 mg/kg; Byk Gulden, Konstanz, Germany), was administered intraperitoneally 2 h before FOP injection.

Analysis of Radiolabeled Metabolites in Tissues

The chemical nature of the metabolites in the liver and heart was analyzed by an extraction procedure as previously described (*17*). The rat tissues were excised 30 min after injection of radiotracer for FTP and 15 min after injection for FOP. Approximately 1 g tissue was thoroughly homogenized and sonicated (20 s) in 7 mL chloroform:methanol, 2:1, at 0°C. Urea (40%, 1.75 mL) and sulfuric acid (5%, 1.75 mL) were added, and the mixture was sonicated for an additional 20 s. After centrifugation for 10 min, aqueous, organic, and protein interphase fractions were separated and counted.

In the case of FOP, the blood serum was analyzed for nonmetabolized FOP. Samples of serum were obtained from blood samples drawn from the left ventricle 20 min after injection of FOP. To 0.3 mL serum was added 0.6 mL MeOH, and the samples were mixed and centrifuged. The supernatant was filtered (13-mm-diameter, 0.2-μm nylon filter) and analyzed for nonmetabolized FOP by analytic reverse-phase HPLC (Econosphere C-18 [5 μm, 250 × 4.6 mm]; Alltech) with the eluent MeOH:water:acetic acid, 85:14.5:0.5, at a flow of 1 mL/min. HPLC eluent samples were continuously collected and counted in a well counter. FOP eluted at 5.8 min. The amount of radioactivity in the samples corresponding to the FOP elution peak was summed and divided by the amount of radioactivity injected. Control samples of nonradioactive serum with added pure FOP were run to account for incomplete recovery of radioactivity during the procedure. The recovery was 92%.

Isolation and Perfusion of Rat Livers

Female Sprague Dawley rats (body weight range, 50–60 g) fasted overnight. After anesthetization with pentobarbital (75 mg/kg) and venous administration of heparin (50 U), the abdominal cavity was opened and the portal vein was cannulated and immediately perfused at a flow of 8 mL/min. The liver (~2–2.5 g wet weight) was then dissected free and placed on a 1.5-cm-diameter grate across the opening of a small funnel. The funnel was then positioned between 2 radioactivity detectors. The perfusion medium was Krebs-Henseleit bicarbonate buffer of the following composition (in mmol/L): Na^+, 143; K^+, 5.9; Ca^{2+}, 1.85; Mg^{2+}, 1.0; Cl^-, 125.6; SO^{2-}_4, 1.18; $H_2PO^-_4$, 1.2; HCO^-_3, 25; glucose, 5; palmitate, 0.15; and albumin, 0.15. The perfusate was prefiltered using 5-μm in-line filters (Millipore). Under standard conditions, the perfusate was gassed with 95% O_2:5% CO_2. To assess the tracer kinetics in conditions of hypoxia, the fraction of oxygen was lowered to 15% while maintaining the CO_2 fraction at 5%. The makeup gas was nitrogen. The apparatus used water-jacketed vessels and a heater–circulator to deliver the medium to the liver at a temperature of 37°C. Perfusion pressure was monitored by a pressure transducer to ensure correct positioning of the cannula. The effluent flow rate was measured manually. The isolated liver was not enclosed in a perfusion chamber, because the ^{18}F radioactivity required close monitoring by external detectors. Therefore, the temperature of the liver was not strictly controlled. The temperature in the livers was presumably nearly the same in all the experiments because the perfusate temperature was maintained at 37°C, the flow was kept constant, and the livers were of similar sizes.

Administration of Radiotracers

For pulse perfusion of radiotracers, 2 reservoirs of perfusate were used. Before each study, 1 reservoir was filled with approximately 500 mL perfusion medium containing 3700–7400 kBq/L [^{18}F]FOP and approximately 1850 kBq/L [9,10-^{3}H]palmitate. A 3-way valve was used for switching the perfusate between the 2 sources. The standard pulse-perfusion protocol consisted of a 20-min stabilization without tracers, a 20-min perfusion with radiotracers, and a 40-min washout (without tracers), in succession.

The ^{18}F radioactivity concentration of the washin medium, R_p (cpm/mL), was measured in a NaI well counter. At the end of perfusion, the liver was gently blotted on paper toweling, sectioned, placed in preweighed tubes, weighed, and counted in the NaI well counter. The liver was later dehydrated in a vacuum oven to obtain the dry mass. The average ratio (±SD) of wet to dry mass of the livers was 4.4 ± 0.4. The apparent distribution volume (ADV) of radioactivity in the whole liver was calculated from the sum of radioactivity in the liver and the paper toweling (A_l), the dry mass of the liver (M_l), and R_p:

$$\text{ADV}\ (t_{end}) = A_l/(R_p \times M_l), \qquad \text{Eq. 2}$$

where t_{end} was the time at the end of perfusion.

Estimation of Oxidation Rate of Exogenous Palmitate

Livers were perfused with [9,10-^{3}H]palmitate at a concentration of 1850 kBq/L. Perfusate samples were collected from the reservoir used to perfuse the liver. Hepatic effluent samples were collected after 10 min of equilibration. Tritiated water and ketone bodies were separated from nonmetabolized ^{3}H-palmitate in the effluent samples by an organic solvent extraction procedure described by Saddik and Lopaschuk (*18*). Fractional palmitate oxidation rate (FPOR) (mL/min/g dry weight) was calculated as the product of perfusate flow (mL/min/g dry weight) and the fraction of concentration of acid-soluble metabolites (tritiated water and ketone bodies) relative to perfusate ^{3}H-palmitate concentration at steady state.

Acquisition and Normalization of ^{18}F Time–Activity Curves in Isolated Rat Livers

^{18}F radioactivity was externally monitored using 2 lead-collimated 5.08 × 5.08 cm (2 × 2 in.) NaI(Tl) scintillation probes configured electronically for γ,γ-coincidence detection. The true coincidence counting rate in the liver (Y_i [counts per second]) was calculated as the difference between prompt coincidence rate and random coincidence rate, with the latter estimated by the delayed-

signal technique. The true coincidence counting rate was corrected for radioactive decay.

For studies in which radiotracers were administered by pulse perfusion, the resultant time–activity curve was converted to units of ADV by multiplication of each data point Y_i by a calibration factor (f_c):

$$ADV_i\ (mL/g\ dry\ weight) = Y_i f_c, \qquad \text{Eq. 3}$$

where f_c is given by the equation:

$$f_c \frac{(mL/g\ dry\ weight)}{(counts\ per\ second)} = \frac{ADV(t_{end})}{Y_e}, \qquad \text{Eq. 4}$$

where $ADV(t_{end})$ is given by Equation 1, and Y_e is the average of Y over the last 10 s of perfusion.

HPLC Analysis of Radioactivity Clearance from Isolated Liver

To determine the contribution of metabolites of FOP to the clearance of radioactivity from the isolated liver, FOP (29.6–37 MBq) was administered to isolated livers as a bolus injection into the perfusion medium at the portal vein. Effluent samples were collected at 0.5–2 min (rapid early phase) and 11–13 min (slower clearance phase) after tracer injection. The effluent samples were processed as previously described for serum samples for analysis by reverse-phase HPLC.

FOP Kinetics in Isolated Rat Liver

The 2-compartment model used for FOP kinetics in isolated rat liver is shown in Figure 2. The first tissue compartment, C_1, is taken to represent radiolabel in the form of nonmetabolized FOP. The second compartment, C_2, is thought to represent turnover of radioactivity within all esterified forms of FOP. Noncovalent binding of FOP or its acyl intermediates to binding proteins within tissue can also contribute to the kinetics of C_2. A blood volume term (BV) was included in the model to account for radiotracer present in the vascular spaces. The potential defluorination of FOP was not explicitly accounted for by the model. Because in vivo defluorination of FOP, as suggested by bone uptake of radioactivity (*19*), was slow relative to the rate of uptake by liver, the errors associated with ignoring this process were likely minimal. Furthermore, we have observed no evidence of defluorination of tracer in human studies (unpublished data, 1999). Potential catabolism of FOP by α-oxidation (*20*) was also ignored in the model.

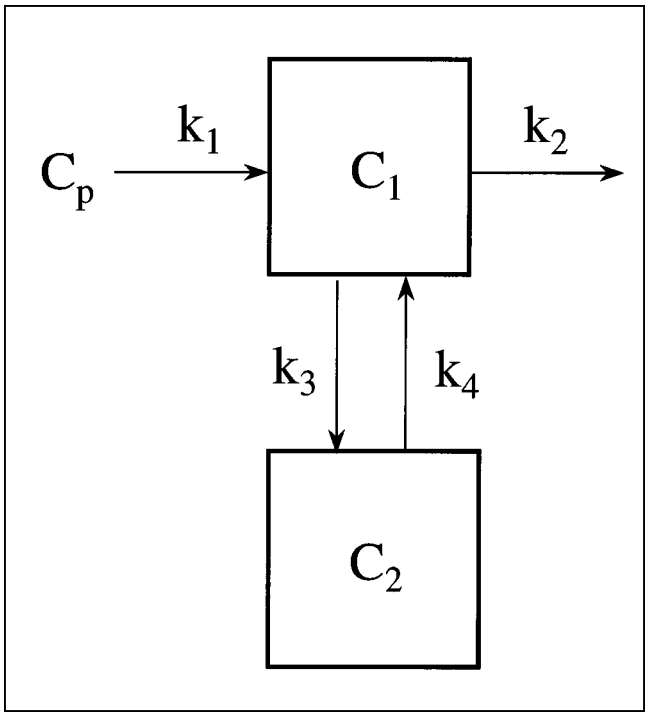

FIGURE 2. Two-compartment model for fitting FOP kinetics in isolated rat liver. C_p is radioactivity concentration in input perfusate; C_1 and C_2 represent first and second tissue compartments, respectively; and k_1–k_4 are rate constants.

The differential equations describing the kinetics of the radiolabel with FOP are:

$$\frac{dC_1(t)}{dt} = k_1 C_p(t) - (k_2 + k_3) C_1(t) + k_4 C_2(t)$$

$$\frac{dC_2(t)}{dt} = k_3 C_1(t) - k_4 C_2(t). \qquad \text{Eq. 5}$$

Because the radioactivity concentration is normalized to the radioactivity concentration in the input perfusate containing FOP (Eq. 3), $C_p(t)$ is given as:

$$C_p(t) = \left\{ \begin{array}{c} 0,\ t < 0 \\ 1,\ 0 \le t \le 20\ min \\ 0,\ t > 20\ min \end{array} \right\}. \qquad \text{Eq. 6}$$

The total ADV of radiolabel in the liver is modeled as:

$$ADV(t) = BV\, C_p(t) + (1 - BV)(C_1(t) + C_2(t)). \qquad \text{Eq. 7}$$

The BV term was not identifiable in the parameter estimation process; BV was therefore fixed to a value of 0.24 mL/g dry weight for all studies to account for tracer present in all vascular spaces in the field of view of the radiation detectors. The compartmental model solutions were derived numerically using a fourth-order Runge-Kutta integrator. Parameter estimation used a nonlinear least squares fitting routine (*21*), minimizing the sum of squares of the differences of measured data and model ADVs for all data points.

The equilibrium distribution volumes (DVs) (equivalent to liver compartment-to-perfusate ratio of FOP concentration at equilibrium) of the model compartments are estimated as:

$$DV_1 = \frac{k_1}{k_2}$$

$$DV_2 = DV_1 \frac{k_3}{k_4} = \frac{k_1 k_3}{k_2 k_4}$$

$$DV_{tot} = DV_1 + DV_2. \qquad \text{Eq. 8}$$

Statistical Analysis

Data are expressed as mean ± SD. The *t* test (2-tailed) for unpaired samples was used to compare the means of 2 groups of samples.

RESULTS

Synthesis of [^{18}F]FOP

FOP was synthesized by no-carrier-added nucleophilic [^{18}F]fluorination of the methyl ester of the corresponding iodo-3-oxa fatty acid, followed by basic hydrolysis and

TABLE 1
Uptake of [^{18}F]FOP in Fasting Rats

Tissue	Control			Etomoxir 15 min (n = 5)
	15 min (n = 5)	30 min (n = 5)	60 min (n = 3)	
Heart	0.023 ± 0.003	0.046 ± 0.003*	0.029 ± 0.005	0.080 ± 0.028*
Blood	0.059 ± 0.007	0.088 ± 0.006†	0.072 ± 0.004*	0.146 ± 0.041†
Lung	0.044 ± 0.008	0.055 ± 0.007	0.041 ± 0.001	0.101 ± 0.037†
Liver	1.531 ± 0.252	1.760 ± 0.110	0.979 ± 0.078†	1.280 ± 0.338
Kidney	0.101 ± 0.031	0.127 ± 0.103	0.066 ± 0.016	0.108 ± 0.029
Bone	0.102 ± 0.032	0.170 ± 0.024†	0.276 ± 0.080†	0.049 ± 0.008*
Brain	0.011 ± 0.031	0.014 ± 0.002	0.013 ± 0.001	0.026 ± 0.010*
Skeletal muscle	0.013 ± 0.003	0.015 ± 0.002	0.017 ± 0.001	0.030 ± 0.007†

*$P < 0.05$ vs. 15-min controls.
†$P < 0.01$ vs. 15-min controls.
Data are % dose kg/g. Control rats were Sprague-Dawley female rats that weighed 180–200 g and had fasted overnight. Etomoxir-treated rats were given 40 mg/kg etomoxir 2 h before tracer injection. Uptake is normalized to body mass (kg).

HPLC purification. The synthesis required approximately 50 min, giving radiochemical yields of 30%–40% (corrected for decay). Hydrolysis of the [^{18}F]fluoroester was quantitative, as evidenced by no radioactive peaks after the elution of FOP on reverse-phase HPLC. No detectable ultraviolet-absorbing (210 nm) material was eluted during the elution of FOP on semipreparatory HPLC. Radiochemical purity was greater than 98% as assessed by analytic reverse-phase HPLC.

Biodistribution and Metabolic Studies in Living Rats

Hepatic uptake of the 3-oxa fatty acid, FOP, was avid (1.76 ± 0.11 % dose kg/g 30 min after injection) (Table 1). Uptake in extrahepatic tissues was less than one tenth that in liver more than 15 min after injection. Figure 3 shows tissue-to-blood ratios for FOP as a function of time during 60 min. The liver-to-blood ratio of FOP was maximal at approximately 15 min, followed by a slow decrease. Heart-to-blood and kidney-to-blood ratios also peaked approximately 15 min after injection, with slow decreases thereafter, whereas bone-to-blood ratios continued to increase over the measurement period. Thus, accumulation of radioactivity in bone was observed with FOP, suggesting slow defluorination of the tracer. Liver uptake was somewhat lower in etomoxir-treated rats, but the difference was not statistically significant (Table 1). However, the concentration of radioac-

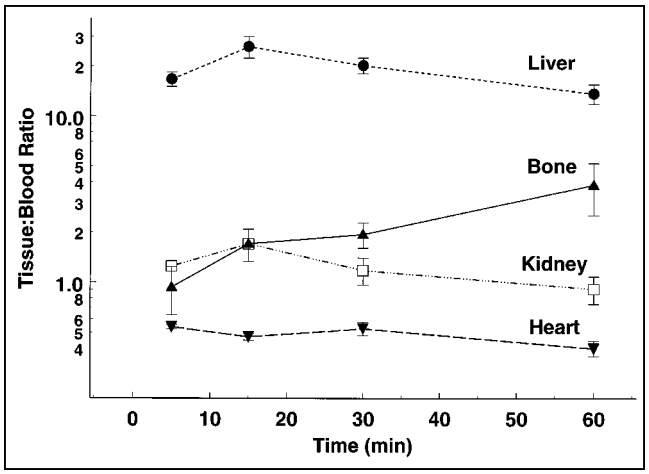

FIGURE 3. Tissue-to-blood ^{18}F radioactivity concentration ratios for FOP in healthy living rats. Each data point represents mean and SD for group of 3–4 rats killed at given time.

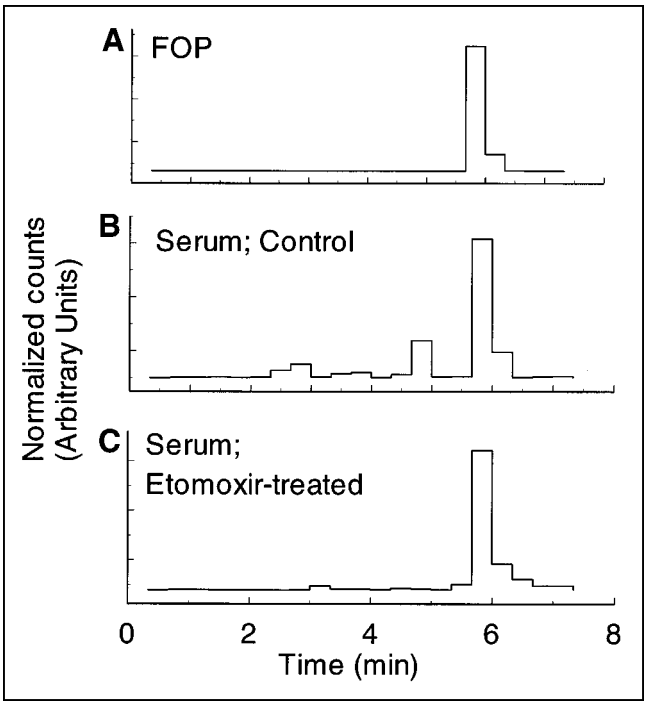

FIGURE 4. Reverse-phase HPLC analysis of FOP standard (A) and ^{18}F radioactivity in representative samples of serum taken from control or etomoxir-treated rats 15 min after injection of FOP (B and C). Small levels of unidentified polar metabolites of FOP were observed in serum samples. Intact FOP composed 85.4% ± 1.4% and 96.7% ± 0.8% ($P < 0.0001$) of total radioactivity in serum 15 min after injection for control and etomoxir-treated rats, respectively.

TABLE 2
Distribution of ^{18}F Radioactivity in Rat Liver In Vivo 15 Minutes After Injection of FOP

Group	Aqueous soluble (%)	Organic soluble (%)	Protein interphase (%)
Control (n = 3)	3.0 ± 0.7	93.3 ± 0.9	3.6 ± 0.1
Etomoxir (n = 3)	6.0 ± 1.6*	88.8 ± 0.4*	4.9 ± 1.4

*$P < 0.05$ vs. control.

tivity in the blood was increased 2.5-fold, so that the liver-to-blood ratio was decreased 64% ($P < 0.0001$) in etomoxir-treated rats (9.5 ± 3.5) in comparison with control rats (26.1 ± 3.8) at 15 min after injection. HPLC analysis of serum (Fig. 4) showed the presence of polar metabolites of FOP; the fraction of nonmetabolized tracer 15 min after injection was 85.4% ± 1.4% and 96.7% ± 0.8% ($P < 0.0001$) for control and etomoxir-treated rats, respectively. However, less than 1% of the injected dose of FOP was found in the urinary bladder at 30 min in control rats, showing FOP and the slowly produced polar metabolites (other than [^{18}F]fluoride) to be effectively reabsorbed by the kidneys. Using only the nonmetabolized FOP concentration in blood, the liver-to-blood ratio was decreased 68% ($P < 0.00005$) with CPT-I inhibition 15 min after injection, from 30.5 ± 4.5 for control rats to 9.8 ± 3.6 for etomoxir-treated rats. Analysis of liver homogenates showed more than 88% of the radioactivity to be organic soluble 15 min after injection for both normal and CPT-I inhibited rat livers (Table 2).

Studies in Isolated Rat Liver

FOP kinetics in isolated rat liver showed rapid and slow turnover (Fig. 5). The rapid process was most apparent in the first 4 min of washout; thereafter, the slower clearance process was evident. The kinetics were successfully fit by a 2-compartment model (Fig. 6), allowing estimation of rate constants k_1–k_4. Table 3 shows the mean values of parameter estimates in normoxic and hypoxic groups. The only rate constant influenced significantly by hypoxia was k_2, which was increased 2.6-fold over normal values. The increase in k_2 with hypoxia translated into decreases of both DV_1 and DV_2, because both DV estimates are inversely proportional to k_2 (Eq. 8). The decreases in DV_1, DV_2, and DV_{tot} with hypoxia tracked closely the 55% decrease in FPOR. The strongest correlation with FPOR was found for k_2, which showed a negative correlation ($k_2 = 0.49 - 0.21 \times$ FPOR,

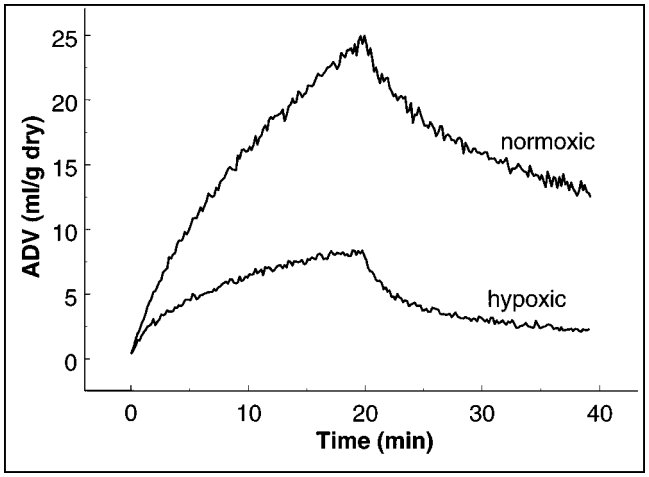

FIGURE 5. Characteristic time–activity curves for FOP in isolated rat livers. Livers were perfused in normoxic (95% O_2) or hypoxic (15% O_2) conditions. Livers were pulse perfused with radiotracer in perfusate at constant concentration over the interval 0–20 min, followed by 20-min washout.

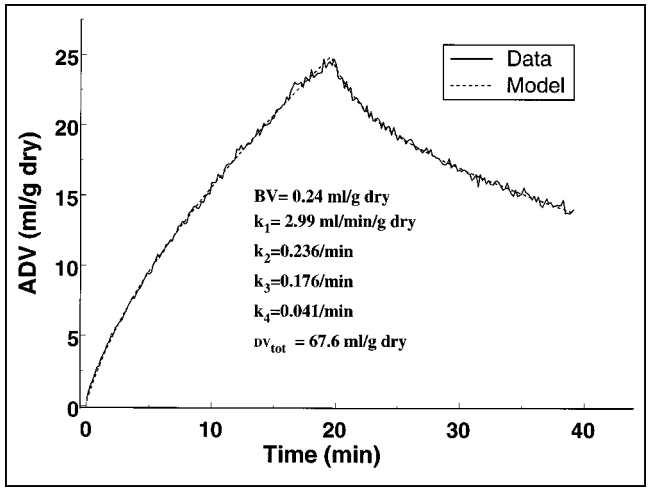

FIGURE 6. Two-compartment model fit to ^{18}F radioactivity kinetics in normoxic isolated rat liver administered FOP as 20-min pulse followed by 20-min washout. Measured kinetics were successfully fit by model, showing no significant discrepancies between data and model curves besides statistical counting noise. k_1–k_4 are rate constants.

TABLE 3
Palmitate Oxidation and FOP Kinetic Parameter Estimates in Isolated Rat Liver

Parameter	Normoxic condition (95% O_2) (n = 5)	Hypoxic condition (15% O_2) (n = 5)	Percentage change
k_1 (mL/min/g dry weight)	2.81 ± 0.49	3.09 ± 0.90	
k_2 (per minute)	0.135 ± 0.046	0.354 ± 0.054	+162*
k_3 (per minute)	0.087 ± 0.045	0.081 ± 0.018	
k_4 (per minute)	0.036 ± 0.010	0.041 ± 0.006	
DV_1 (mL/g dry weight)	22.9 ± 8.6	9.0 ± 3.3	−61†
k_3/k_4	2.30 ± 0.91	2.04 ± 0.54	
DV_2 (mL/g dry weight)	47.2 ± 10.5	18.1 ± 7.6	−62‡
DV_{tot} (mL/g dry weight)	70.1 ± 13.9	27.2 ± 10.3	−61‡
Fractional palmitate oxidation rate (mL/min/g dry weight)	1.31 ± 0.30	0.587 ± 0.080*	−55†

*$P < 0.0001$, vs. normoxic.
†$P < 0.01$, vs. normoxic.
‡$P < 0.0005$, vs. normoxic.

$r = 0.70$), suggesting faster backdiffusion of tracer from compartment 1 as FPOR was decreased. The DVs of the compartments are shown in Figure 7 as a function of FPOR. The DVs of both compartments correlated positively with FPOR because both DVs were inversely related to k_2. The strongest relationship was found for the DV of the slower compartment: DV_2 (mL/g dry weight) = 34.1 FPOR (mL/min/g dry weight) − 0.7 ($r = 0.89$). The intercept of this linear fit was not significantly different from zero. The total DV, given by the sum of the 2 compartmental DVs, showed a nonlinear relationship with FPOR (Fig. 7). The relative noise appeared to be smaller for DV_2 and DV_{tot} estimates in comparison with DV_1 (Fig. 7).

To determine the contributions of intact FOP and metabolites to the clearance of radioactivity from isolated livers, we performed separate studies with bolus injections of FOP (29.6–37 MBq) to isolated livers perfused in normoxic and hypoxic (15% O_2) conditions. HPLC analysis was performed on effluent samples to determine the fraction of nonmetabolized FOP during the rapid early (0.5–2 min) and slower late (11–13 min) clearance phases (Table 4). Intact FOP accounted for 66%–69% and 90%–91% of the radioactivity clearing normoxic and hypoxic livers, respectively, over both early and late clearance phases. Thus, metabolism of FOP to diffusible radiolabeled metabolites was significantly greater in normoxic conditions. Only samples from the late phase in normoxic livers showed significant levels of radioactivity (14%) retained on the C-18 HPLC column. The chemical form of this fraction of radioactivity was likely [^{18}F]fluoride, which is nearly completely retained on the column under these conditions. Slow defluorination of FOP in the normoxic liver is also consistent with the observed moderate uptake by bone of radioactivity in living rats. In contrast, there was no evidence of defluorination of FOP in hypoxic liver consistent with decreased availability of oxygen and of energy equivalents that are required for ω-oxidation. The FOP metabolites that were not retained on the C-18 column, accounting for as much as 30% of the clearance in the rapid early phase in normoxic livers, were not chemically identified.

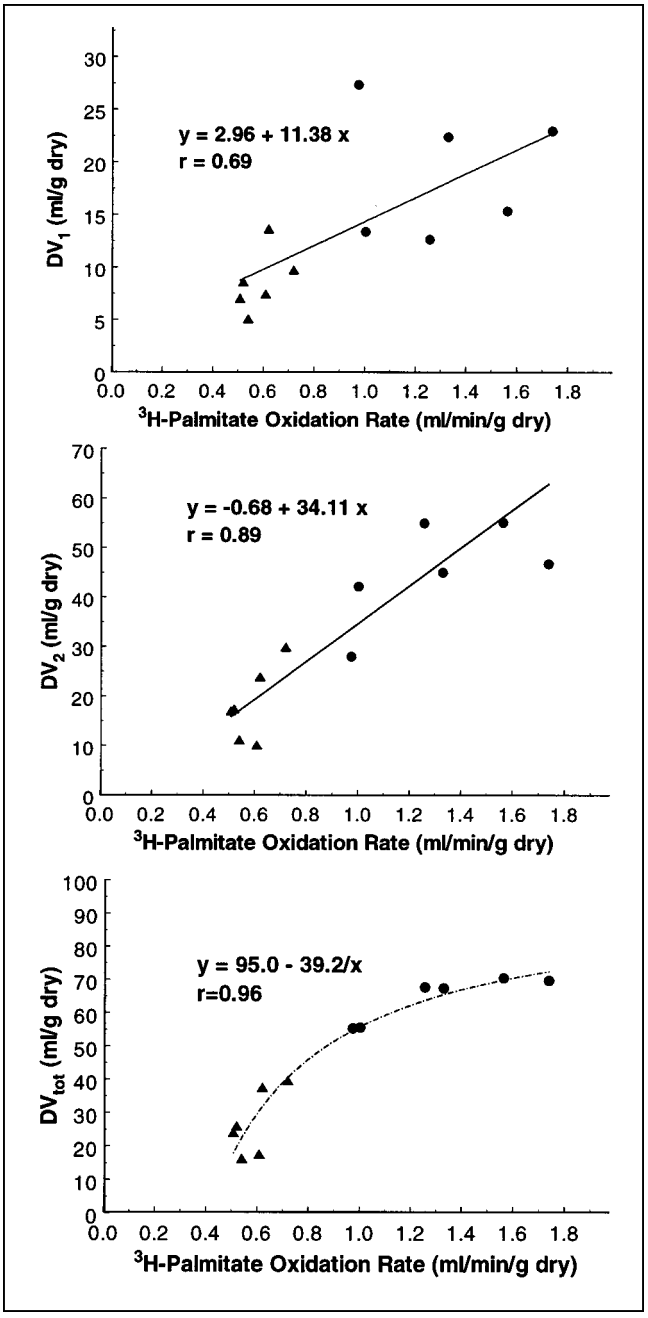

FIGURE 7. Relationship of estimates of DVs of FOP to FPOR in isolated rat liver. Each experiment is represented by single data point on each graph. Both normoxic (95% O_2) data (●) and hypoxic (15% O_2) data (▲) are shown.

DISCUSSION

Noninvasive assessment of regional HMFAO in liver may help to clarify the pathogenesis of liver diseases and may be useful in clinical diagnosis. The deleterious effects of ethanol on mitochondrial oxidative function in liver have been extensively studied (*1*,*22*,*23*). However, the potential role of mitochondrial dysfunction has not been clarified in NASH (*2*). Evaluating HMFAO disorders is also of interest in obesity (*3*,*4*) and type II diabetes (*5*,*6*). Abnormally high triglyceride accumulation in hepatocytes may result from impairment of β-oxidation of fatty acids because of disturbances of mitochondrial oxidative metabolic function. Thus, a noninvasive means of assessing hepatocyte mitochondrial β-oxidation in vivo not only could prove useful diagnostically but also might be of use for judging the severity (i.e., prognosis) of disease.

In this study, we evaluated the usefulness of FOP as a PET tracer of fatty acid oxidation in liver. FOP incorporates an oxygen heteroatom substitution to obstruct β-oxidation of the molecule and thereby simplify the interpretation of the externally detected kinetics in liver. The choice of substituting the oxygen atom at C3 for FOP was guided by work of Skorve et al. (*12*) that studied [1-^{14}C]palmitoyl-carnitine oxidation in liver mitochondria procured from rats fed

TABLE 4
HPLC Analysis of Effluent Samples from Isolated Rat Liver with FOP

Group	Intact FOP (%)	Eluted metabolites (%)	Retained metabolites (%)
Normoxic (n = 3)			
Early (0.5–2 min)	69.0 ± 10.3	30.5 ± 9.7	0.5 ± 2.2
Late (11–13 min)	66.0 ± 14.1	20.2 ± 13.3	13.8 ± 1.2*
Hypoxic (n = 3)			
Early (0.5–2 min)	91.4 ± 1.0†	9.1 ± 1.7†	−0.5 ± 2.1
Late (11–13 min)	89.7 ± 5.6†	8.8 ± 4.8†	1.0 ± 2.3†

*$P < 0.0001$ vs. early phase.
†$P < 0.01$ vs. normoxic.
FOP was administered to livers as bolus. Effluent was sampled during washout of radioactivity from livers over early and late intervals given in table. HPLC conditions were as given in Materials and Methods. Fractions of radioactivity as intact FOP, eluted metabolites, and metabolites retained on C-18 HPLC column (obtained by balance of first 2) are given.

pharmacologic doses of nonfluorinated 3-oxa or 4-oxa fatty acids. β-oxidation was more than 97% inhibited in the group fed 3-oxa fatty acids. In contrast, feeding of the 4-oxa fatty acids had no effect on palmitoyl-carnitine oxidation in liver mitochondria (*12*). The mechanisms underlying these differences were not clarified, but a metabolite of the 3-oxa fatty acid likely accumulated in the mitochondrion and caused the inhibition of β-oxidation at 1 or more steps beyond the CPT-I step (carnitine acylcarnitine-translocase, CPT-II, very-long-chain dehydrogenase, mitochondrial trifunctional protein, etc.). The accumulation of a radiolabeled 3-oxa fatty acid in liver was anticipated to potentially serve as a marker of mitochondrial oxidative metabolism of fatty acids.

FOP is taken up avidly by liver in the living rat. The high ratio of ^{18}F radioactivity concentration in liver relative to the concentration of intact FOP in blood (30.5:1) provides evidence of a mechanism of binding or metabolic retention of the tracer in tissue. Comparison of data from our laboratory in the same isolated rat liver model using the 4-thia tracer, FTP (*10*), suggests a slower intracellular sequestration of FOP relative to FTP, consistent with the observed 50% slower rate of activation of 3-oxa-heptadecanoic acid relative to a 4-thia-stearic acid by in vitro assay (*24*). The much lower uptake of FOP in heart relative to myocardial uptake of palmitate (*25*) or 4- and 6-thia fatty acid analogs (*9,10,17*) is intriguing. Differences in activities of enzymes and carriers of fatty acid use in liver and heart for the 3-oxa fatty acid are implicated. Two isoforms of CPT-I are known to exist; one is predominant in liver and the other in heart (*26*). The liver form of CPT-I may have greater activity with 3-oxa fatty acids than does the heart form. Alternatively, differences in molecular specificities of long-chain acyl-CoA synthetase could be present in heart and liver, or acyl-CoA or acylcarnitine hydrolases may be more prevalent in heart and therefore result in more prominent clearance of 3-oxa fatty acids from myocytes.

FOP uptake kinetics in liver are reversible (Fig. 5). Consequently, the most appropriate index of FOP kinetics for assessment of HMFAO appears to be equilibrium DV of the tracer in liver. DV is equivalent to the liver-to-plasma radioactivity concentration ratio at equilibrium if the concentrations of radiolabeled compounds in both arterial and venous plasma are equal and the presence of radiolabeled metabolites other than FOP in plasma are negligible. If radiolabeled metabolites are present in the plasma in human studies, then their potential uptake by liver will need to be characterized and accounted for. Liver-to-blood ratios of FOP showed good sensitivity to impairment of fatty acid oxidation by CPT-I inhibition in living rats. Furthermore, experiments in isolated rat liver showed DV estimates, particularly of the slower turnover compartment (DV_2), to track the fatty acid oxidation rate in the liver. The measurement of the tissue-to-blood (or tissue-to-plasma) ratio with FOP in humans with PET would be straightforward using images of the liver and arterial blood concentration from the left ventricular blood pool after equilibrium is reached. Because of the slow metabolism of the tracer relative to circulatory turnover, venous blood samples could likely be used for measurements of nonmetabolized fraction of tracer in the plasma. Use of a tissue-to-blood ratio as an index of HMFAO would obviate tracer kinetic modeling of dynamic PET image data for estimation of rate constants. A compartmental model–based technique would be complicated because the liver has both arterial and venous perfusion sources in vivo that are distributed in different proportions over the entire liver. However, the model-independent tissue-to-blood ratio cannot distinguish the contributions to the DV of kinetically distinct compartments, as can be accomplished with the isolated rat liver model.

The correspondence of the 2 compartments in the tracer kinetic model to transport and metabolic processes for FOP in liver has not been clarified. Because the 3-oxa fatty acid is not a substrate for β-oxidation, the primary expected radiolabeled metabolites of FOP in liver are the esterification products—FOP-CoA and FOP-carnitine—and complex lipids, whereas [^{18}F]fluoride may be produced as a result of microsomal ω-oxidation (*19*). Another possibility is that peroxisomal α-oxidation (*20*) or microsomal peroxidation (*27*) of the tracer may occur slowly over time. The finding of nearly all the radioactivity in the organic-soluble fraction of liver extracts shows that FOP is not significantly metabolized to hydrophilic metabolites. Although slow accumulation of radioactivity was observed in bone of the rat with FOP, we have observed bone uptake of radioactivity with neither FTP (*9*) nor FOP in humans (unpublished data, 1999). These data suggest that the ω-oxidative defluorination of ω-[^{18}F]fluoro–fatty acid tracers apparent in rodents (*19*) is an insignificant process in humans. Clearance of radiolabeled metabolites produced in liver and other tissues could explain the presence of metabolites in blood and the decline of the liver-to-blood ratio over time.

If present in rat liver homogenates, the CoA ester of FOP

would be expected to distribute primarily in the protein interphase layer (*28*). The minimal amount of radioactivity in the protein interphase layer of liver homogenates 15 min after FOP injection (Table 2) therefore suggests that FOP-CoA may be an intermediate through which FOP is metabolized, but the equilibrium DV of FOP-CoA is relatively small. This finding also implies that if formed in the mitochondrion, FOP-CoA does not significantly accumulate but is either hydrolyzed or transesterified. These results may have some relevance to the finding of potent inhibition of β-oxidation of palmitoyl-carnitine in liver mitochondria from rats fed 3-oxa fatty acids (*12*). The mechanism of inhibition may not involve accumulation of the 3-oxa-acyl-CoA esters in the mitochondrion.

Presuming that FOP is converted to its carnitine ester (FOP-carnitine) in liver and other tissues, the equilibration of FOP and FOP-carnitine between blood and tissues is a plausible explanation for the observed biodistribution in the living rat apart from the accumulation of radioactivity in bone. Cytoplasmic long-chain acylcarnitines are exchangeable with extracellular acylcarnitines, and changes in intracellular acylcarnitine levels are reflected by corresponding changes in plasma acylcarnitine levels (*29*,*30*). The minimal excretion of radioactivity into the urine is consistent with reabsorption of long-chain acylcarnitines by the kidneys (*31*,*32*). Thus, at least 1 of the unidentified polar lipid metabolites of FOP observed in blood serum samples of the rat could be FOP-carnitine. In the CPT-I–inhibited animal, acylcarnitine formation is blocked and long-chain fatty acid levels rise in liver cytosol and plasma, and esterification of fatty acids to form complex lipids, particularly triglycerides, is enhanced (*33*). The findings of dramatically lower levels of polar lipid metabolites of FOP in serum (Fig. 4) and reduced liver-to-blood ratios in CPT-I–inhibited rats (Table 1) may reflect lower production of FOP-carnitine in liver with CPT-I inhibition.

The clearance rate of the most rapid process (estimated by k_2 in the FOP 2-compartment model) was the parameter most sensitive to the effects of hypoxia on fatty acid metabolism in the isolated liver. This rate showed an inverse relationship with β-oxidation activity in the liver. HPLC analysis of effluent samples showed this process to predominantly represent backdiffusion of intact FOP. Enhanced backdiffusion of the tracer from liver in hypoxia can be attributed to 1 or more of the following factors that lower the rate of activation of FOP in the hepatocyte and thereby promote backdiffusion: a decrease in HMFAO leading to accumulation of fatty acyl-CoAs, which cause product inhibition of FOP activation; a decrease of the cytosolic adenosine triphosphate level; and an increase in nonesterified fatty acid concentrations in the cytoplasm leading to competitive inhibition of FOP activation. The slow clearance of FOP was also found to primarily reflect clearance of intact tracer from the liver, presumably reflecting turnover of FOP in esterified forms or intracellular compartments within hepatocytes. Thus, the initial metabolic data suggest that the putative 2-compartment model is adequate for the modeling of FOP kinetics in liver, with the exception of not strictly accounting for a relatively low production of unidentified metabolites. The fraction of radiolabeled metabolites of FOP in late effluent samples (~30%) from normoxic perfused liver was higher than that found in serum of control rats 15 min after injection (~15%). This discrepancy can be explained by differences in hepatic use of FOP in ex vivo versus in vivo liver, differential uptake of metabolites (i.e., [^{18}F]fluoride by bone) in extrahepatic tissues in the living animal, or differences between nonequilibrium washout (ex vivo) versus quasiequilibrium (in vivo) conditions. The influence of metabolism of FOP, if independent of β-oxidation activity, would depend on the clearance kinetics of the product metabolites and the relationship of metabolic rate to β-oxidation activity. From our data on perfused rat liver, the formation of metabolic products of FOP is markedly reduced in hypoxia, suggesting that the auxiliary metabolic process requires oxygen or energy equivalents in correspondence with the requirements of β-oxidation.

Biliary clearance of FOP was not separately estimated in this study. Biliary excretion can influence the results by decreasing the ADV of tracer in the liver. We did not anticipate biliary excretion of the long-chain fatty acid tracers because it is known to be a negligible process for such tracers. Indeed, imaging studies in humans with FOP (unpublished data, 1999) showed no evidence of biliary excretion of this tracer.

Conceptually, the 4-thia and 3-oxa fatty acids may probe fatty acid oxidation by different mechanisms. A metabolic trapping scheme has been proposed for the 4-thia analog as developed in an earlier study with the 6-thia fatty acid, 14-[^{18}F]fluoro-6-thia-heptadecanoic acid, in heart (*17*). By this approach, a PET-derived estimate of the rate of production of well-retained oxidative metabolites of FTP in tissue may serve as a quantitative index of fatty acid oxidation rate. This approach has met initial success with ^{18}F-labeled 4-thia fatty acids in heart because the retention of radioactivity appears to specifically trace the β-oxidation pathway, even in conditions of hypoxia (*9*,*10*). However, the trapping of FTP in liver is not as selective as in heart for the mitochondrial β-oxidation pathway (*11*). Because 3-oxa fatty acids presumably cannot have β-oxidation metabolites, the indication of fatty acid oxidation rate with FOP is less direct than for the metabolic trapping approach. The data from this study suggest that the DV of FOP may serve as an index of mitochondrial β-oxidation activity in liver. The DV of FOP, as measured at an early time point on equilibration with blood (15–30 min), is presumably determined by a complex relationship. This relationship includes fatty acid oxidation rate, delivery of fatty acids, intracellular lipolysis rates, concentrations of hormones, and cofactors and modulators of the multiple enzymes and carriers necessary for activation and transport of fatty acids into the mitochondrion. Also included are flux of competing pathways for acyl-CoAs and acylcarnitines; concentrations of competing acyl-CoAs and

acylcarnitines at CPT-I, carnitine acylcarnitine translocase, and CPT-II; and hydrolysis rates of acyl-CoA and acylcarnitine. Lipolysis of intracellular lipid (e.g., triglyceride) stores creates an alternative source of fatty acids for oxidation in mitochondria. FOP uptake in liver presumably traces HMFAO from exogenous fatty acids. Endogenous contributions to the total HMFAO may be an important variable to consider in situations in which endogenous lipolysis rates are significant.

CONCLUSION

FOP shows promise as a PET tracer of mitochondrial oxidative metabolism of exogenous long-chain fatty acids in liver using facile measurements of its equilibrium DV in tissue (tissue-to-blood ratio). Hepatic uptake kinetics are relatively rapid and reversible. The equilibrium DV in isolated rat liver tracks the decrease in β-oxidation rate of exogenous palmitate induced by hypoxia. FOP undergoes slow metabolism in the rat to unidentified polar lipid species and free [^{18}F]fluoride. Further studies are required to clarify the biochemical fate of FOP in liver and determine its general applicability as a PET probe of regional HMFAO.

ACKNOWLEDGMENTS

This study was supported by grant HL-54882 of the National Institutes of Health, Bethesda, MD. Etomoxir was generously provided by Dr. H. Wolf of Byk Gulden, Konstanz, Germany.

REFERENCES

1. Eaton S, Record CO, Bartlett K. Multiple biochemical effects in the pathogenesis of alcoholic fatty liver. *Eur J Clin Invest.* 1997;27:719–722.
2. Sheth SG, Gordon FD, Chopra S. Nonalcoholic steatohepatitis. *Ann Intern Med.* 1997;126:137–145.
3. Kahler A, Zimmermann M, Langhans W. Suppression of hepatic fatty acid oxidation and food intake in men. *Nutrition.* 1999;15:819–828.
4. Scharrer E. Control of food intake by fatty acid oxidation and ketogenesis. *Nutrition.* 1999;15:704–714.
5. Sidossis LS, Mittendorfer B, Walser E, Chinkes D, Wolfe RR. Hyperglycemia-induced inhibition of splanchnic fatty acid oxidation increases hepatic triacylglycerol secretion. *Am J Physiol.* 1998;E798–E805.
6. Randle PJ, Priestman DA, Mistry S, Halsall A. Mechanisms modifying glucose oxidation in diabetes mellitus. *Diabetologia.* 1994;37(suppl 2):S155–S161.
7. Yamamura N, Magata Y, Kitano H, Konishi J, Saji H. Evaluation of [1-^{11}C]octanoate as a new radiopharmaceutical for assessing liver function using positron emission tomography. *Nucl Med Biol.* 1998;25:467–472.
8. Kawashima H, Kuge Y, Yajima K, Miyake Y, Hashimoto N. Development of step-specific PET tracers for studying fatty acid β-oxidation: biodistribution of [1-^{11}C]octanoate analogs in rats and a cat. *Nucl Med Biol.* 1998;25:543–548.
9. DeGrado TR, Wang S. An F-18 labeled probe of fatty acid oxidation for use with positron emission tomography (PET) [abstract]. *FASEB J.* 1999;13:A764.
10. DeGrado TR, Wang S, Holden JE, Nickles RJ, Stone CK. Synthesis and preliminary evaluation of ^{18}F-labeled 4-thia palmitate as a PET tracer of myocardial fatty acid oxidation. *Nucl Med Biol.* 2000;27:221–231.
11. DeGrado TR, Wang S, Rockey DC. Evaluation of ^{18}F-labeled 16-fluoro-4-thia-palmitate (FTP) as a PET tracer for β-oxidation of long-chain fatty acids in liver [abstract]. *J Nucl Med.* 1999;40(suppl):124P.
12. Skorve J, Asiedu D, Solbakken M, Gjestdal J, Songstad J, Berge RK. Comparative effects of oxygen and sulfur-substituted fatty acids on serum lipids and mitochondrial and peroxisomal fatty acid oxidation in rat. *Biochem Pharmacol.* 1992;43: 815–822.
13. Sonnet PE, Proveaux AT, Adamek E, Sugie H, Sato R, Tamaki Y. Stereoisomers and analogs of 14-methyl-1-octadecene, sex pheromone of peach leafminer moth, *Lyonetia clerkella*, L. *J Chem Ecol.* 1987;13:547–555.
14. Nagatsugi F, Sasaki S, Maeda M. Synthesis of ω-fluorinated octanoic acid and its β-substituted derivatives. *J Fluorine Chem.* 1992;56:373–383.
15. DeGrado TR. Synthesis of 14(R,S)-[^{18}F]fluoro-6-thia-heptadecanoic acid (FTHA). *J Label Comp Radiopharm.* 1991;29:989–995.
16. Coenen HH, Klatte B, Knoechel A, Shueller M, Stoecklin G. Preparation of N.C.A. [17-^{18}F]fluoroheptadecanoic acid in high yields via aminopolyether supported, nucleophilic fluorination. *J Label Comp Radiopharm.* 1986;23:455–466.
17. DeGrado TR, Stöcklin G, Coenen HH. 14(R,S)-[^{18}F]fluoro-6-thia-heptadecanoic acid (FTHA): evaluation in mouse of a new in vivo probe of myocardial utilization of long-chain fatty acids. *J Nucl Med.* 1991;32:1888–1896.
18. Saddik M, Lopaschuk G. Myocardial triglyceride turnover during reperfusion of isolated rat hearts subjected to a transient period of global ischemia. *J Biol Chem.* 1992;267:3825–3831.
19. DeGrado TR, Moka DC. Non-β-oxidizable ω-[^{18}F]fluoro long-chain fatty acid analogs show cytochrome P-450 mediated defluorination: implications for the design of PET tracers of myocardial fatty acid utilization. *Nucl Med Biol.* 1992;19:389–397.
20. Mihalik SJ, Rainville AM, Watkins PA. Phytanic acid alpha-oxidation in rat liver peroxisomes: production of alpha-hydroxyphytanoyl-CoA and formate is enhanced by dioxygenase cofactors. *Eur J Biochem.* 1995;232:545–51.
21. Marquardt DW. An algorithm for least-squares estimation of nonlinear parameters. *J Soc Ind Appl Math.* 1963;11:431–441.
22. Williamson JR, Scholz R, Browning ET, et al. Metabolic effects of ethanol in perfused rat liver. *J Biol Chem.* 1969;244:5044–5054.
23. Cederbaum AI, Lieber CS, Beattie DS, et al. Effect of chronic ethanol ingestion on fatty acid oxidation by hepatic mitochondria. *J Biol Chem.* 1975;250:5122–5129.
24. Aarsland A, Berge RK. Peroxisome proliferating sulphur- and oxy-substituted fatty acid analogues are activated to acyl coenzyme A thioesters. *Biochem Pharmacol.* 1991;41:53–61.
25. Elmaleh DR, Livni E, Levy S, Varnum D, Strauss HW, Brownell GL. Comparison of ^{11}C and ^{14}C-labeled fatty acids and their β-methyl analogs. *Int J Nucl Med Biol.* 1983;10:181–187.
26. Weis BC, Cowan AT, Brown N, Foster DW, McGarry JD. Use of a selective inhibitor of liver carnitine palmitoyltransferase I (CPT I) allows quantification of its contribution to total CPT I activity in rat heart. *J Biol Chem.* 1994;269:26443–26448.
27. Esterbauer H, Benedetti A, Lang J, Fulceri R, Fauler G, Comporti M. Studies on the mechanism of formation of 4-hydroxynonenal during microsomal lipid peroxidation. *Biochim Biophys Acta.* 1986;876:154–166.
28. Rosendal J, Knudsen J. A fast and versatile method for extraction and quantification of long-chain acyl-CoA esters from tissue: content of individual long-chain acyl-CoA esters in various tissues from fed rat. *Anal Biochem.* 1992;207:63–67.
29. Pande SV, Parvin R. Clofibrate enhancement of mitochondrial carnitine transport system of rat liver and augmentation of liver carnitine and gamma-butyrobetaine hydroxylase activity by thyroxine. *Biochim Biophys Acta.* 1980;617:363–70.
30. Bhuiyan AKMJ, Jackson S, Turnbull DM, Aynsley-Green A, Leonard JV, Bartlett K. The measurement of carnitine and acyl-carnitines: application to the investigation of patients with suspected inherited disorders of mitochondrial fatty acid oxidation. *Clin Chim Acta.* 1992;207:185–204.
31. Steinmann B, Bachmann C, Colombo JP, Gitzelmann R. The renal handling of carnitine in patients with selective tubulopathy and with Fanconi syndrome. *Pediatr Res.* 1987;21:201–204.
32. Sugimoto T, Nishida N, Woo M, et al. Serum and urinary carnitine and organic acids in Reye syndrome and Reye-like syndrome. *Brain Dev.* 1986;8:257–261.
33. Wolf HPO, Eistetter K, Ludwig G. Phenylalkyloxirane carboxylic acids, a new class of hypoglycaemic substances: hypoglycaemic and hypoketonaemic effects of sodium 2-[5-(4-chlorophenyl)-pentyl]-oxirane-2-carboxylate (B807–27) in fasted animals. *Diabetologia.* 1982;22:456–463.